Proceedings of the 2013

International Conference on

Computational and Mathematical

Methods in Science and Engineering

Almería, Spain

June 24-27, 2013

CMMSE

VOLUME II

Editors: Ian Hamilton & Jesús Vigo-Aguiar

Associate Editors:

H. Adeli, P. Alonso, M.T. De Bustos, M. Demiralp, J.A. Ferreira, A. Q. M. Khaliq,

J.A. López-Ramos, P. Oliveira, J.C. Reboredo, M. Van Daele,

E. Venturino, J. Whiteman, B. Wade

ISBN 978-84-616-2723-3

Printed on acid-free paper

Proceedings of the 13th International Conference
on Computational and Mathematical Methods
in Science and Engineering, CMMSE 2013
24–27 June, 2013.

Power Spectral Density estimation of ELF signals by averaged of Periodograms

Manuel Fernández Ros[1], Jose Antonio Gázquez Parra[2], Nuria Novas Castellano[2] and Rosa García Salvador[2]

[1] *Consejería de Educación, Andalusian Regional Government*

[2] *Department of Engineering, University of Almería*

emails: manuelfr@ieselargar.org, jgazquez@ual.es, nnovas@ual.es, rgs768@ual.es

Abstract

The set formed by the earth's crust and the inner edge of the ionosphere form a resonant cavity where there is electrical activity due to atmospheric phenomena such as rays, giving rise to electromagnetic signals into the ELF band. The interest in studying the electromagnetic activity in the ELF band lies in the possibility to establish a correlation between them and the conditions environment as a diagnostic method of the environment.

For that analysis we'll use the averaged periodogram methods based on the Fast Fourier Transform (FFT) for estimating the spectral density power (PSD). Thus we give the needed information about the best time of capture, the length of segments and the number of averages.

Key words: ELF, resonant cavity, PSD, transform, density, spectral, power, Schumann, periodogram

1 Introduction

In 2011 started the operations of the observatory of electromagnetic waves Extremely Low Frequency [1], located on the area of the Calar Alto in the province of Almería, Spain. The observatory is equipped with two magnetometers oriented NS and EW directions, focused to electromagnetic capture signals in the ELF band.

This frequencies band, ranging from 0.03 Hz to 300 Hz, and was introduced in Recommendation ITU-R V.431 at the request of the URSI (International Union of Radio Science),

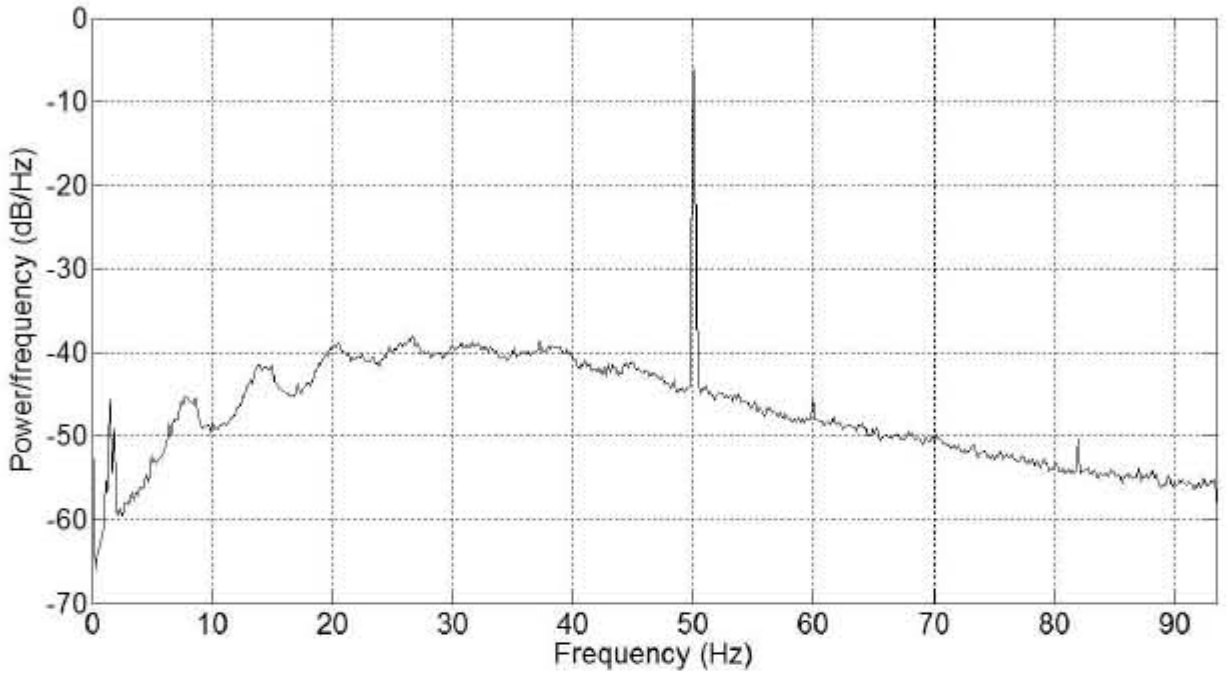

Figure 6: $Tc = 30$', $L = 336600$, $M = 1870$, $K = 180$.

5 Conclusions

In view of the results obtained by averaging the periodograms we can conclude that in the case of study of the Schumann resonances characterized by wide band signals where we only intended to detect the amplitude and position of the center frequency of the resonance, it is enough to work with short data records (2 minutes), with segments also reduced (187 samples) and a relatively small number of periodograms (120).

In the case of narrow-band signals it is required to have access to the carrier as well as the information of modulation signals, and to do so it is needed a resolution of 0.01 Hz, that leadd to increase the length of the segments (1870 samples or more) in order to increase the resolution in frequency.

Acknowledgements

This work was supported in part by the Ministry of Innovation, Science and Enterprise (Andalusian Regional Government and Central Government) under Project FQM-32080, TEC2009-13763-C02-02 and in part by the European Union FEDER Program, as part of the "Electronics, Communications and Telemedicine" (TIC-019) Research Group of the University of Almeria.

References

[1] International Telecommunication Union. *Recommendation ITU-R V.431-7: Nomenclature of the frequency and wavelength bands used in telecommunications.*

[2] A.P. Nickolaenko. Intensity of schumann resonance: Universal time and local time variations. *Conf. On Symposium proceedings. MSMW'07, kharkov, Ukraine*, 2007.

[3] A.P. Nickolaenko;M. Hayakawa;Y. Hobara. Schumann resonances and global lightning activity, mathematical methods in electromagnetic theory. *Proceedings of MMET'98 Conference*, vol. 1, 1998.

[4] M. Hayakawa;R. Kawate;O. Molchanov. Results of ultra-low-frequency magnetic field measurements during the guan earthquake of 8 august 1993. *Geophysics Research Letters*, vol. 23, 1996.

[5] K. Ohta;N. Watanable;M. Hoyakawa. Survey of anomaluous schumann resonance phenomena observed in japan, in possible association with earthquakes in taiwan. *Physical and chemistry of the Earth*, vol. 31(4-9):pp. 397–402, May 2006.

[6] M. Fullekrug; A.C. Fraser-Smith. Further evidence for a global correlation of the earth-ionosphere cavity resonances. *Geophisical Research Letters*, vol. 23(20):pp. 2773–2776, October 1996.

[7] Peter D. Welch. The use of fast fourier transform for the estimation of power spectra: A method based on time averaging over short, modified periodograms. *IEEE Transactions on Audio and Electroacoustics*, AU-15(2), 1967.

[8] John G. Proakis y Dimitris G. Manolakis. *Tratamiento digital de señales.*

[9] Sir Arthur Schuster. On the investigation of hidden periodocities with application to a supposed twenty-six-day period of meteorological phenomena. *Journal of Geophysical Research*, vol. 3(20):pp. 13 –41, March 1898.

[10] M.S. Bartlett. Smoothing periodograms from time series with continuous spectra. *Nature*, vol. 161, 1948.

[11] O. Rompelman; H.H. Ros. Coherent averaging and the equivalent filter review. part 1: Noise reduction and the equivalent filter. *Journal of Biomedical Engineering*, vol. 8, 1986.

and particularly those known as Schumann Resonances: 7 Hz fundamental frequency, and modes of 14 Hz, 21 Hz, 28 Hz, 35 Hz, 42 Hz, and 49 Hz. These resonances appear as broad-band signals over radio noise. Several papers suggest that these frequencies are not constant and can vary with geographical location (land, sea, temperate or cold climates, time of day) [2], state of the ionosphere and atmosphere. Moreover these data serve as a reference for the measurement of thunderstorm activity [3] and seismic activity [4][5], hence the interest in the determines the level and frequency of the resonances and relates it with the diagnosis of the environment.

Other signals within this band, of human origin, are those for maritime communications with underwater submarines [6] which appear as narrow-band signals.

The instrumentation of the measuring station, is composed by magnetic field sensors, based on large coils core, instrumentation amplifier with very low noise and system acquisition and digital conversion ADC 24-bit high resolution, running with oversampling technique. Data obtained directly from the converter are subjected to a decimation process in frequency, by averaging in the time domain, without loss of information and to reduce noise acquisition.

Finally the data are sent in real time to processing and storage center at the University of Almería, with the purpose of processing by spectral estimation techniques power. By using these techniques, the data are subjected to spectral averaging process to observe phenomena undetectable initially. This implies some loss of information, because it is assumed that the information is the same in each spectral window and these signals actually vary with time.

This paper addresses the technique of power spectral estimation based on periodogram averaging method, provided by Welch [7].

2 Espectral estimation

Signals from physical processes in general belong to signals of stationary random processes. Such signals have not finite energy, but have finite average power, so for its study, we use the power spectral density, or PSD. Of course when we refer to *signals*, we mean sampled signals $x(n)$. This has profound implications because we will not have infinite data records, $(-\infty < n < \infty)$, but only a portion of length N, $(0 \leq n \leq N-1)$, which leads us to introduce the concept of time windows.

There are two basic methods of spectral estimation, the direct and indirect:

- Direct method: consists in the calculation of the Fourier Transform of the signal.
- Indirect method: Its name comes from the fact that it is made in two steps:
  1. Calculating the autocorrelation of the signal.
  2. Fourier transform of the autocorrelation, that gives the spectral density.

 ISBN: 978-84-616-2723-3

This set of methods are also called *non-parametric methods*, in reference to not need a prior knowledge about the origin of the signal, or process that creates it. As we have advanced, the base is the Discrete Fourier Transform or DFT, estimated using any of the efficient algorithms, based on the Fast Fourier Transform (FFT). These methods have the drawback of requiring long data records in order to obtain high resolution in the frequency. On the other hand, the use of registers with high number of samples, increases the spectral spill phenomenon, leading to the occurrence of false frequencies. [8].

2.1 The Periododram

The signals caused by stationary random processes have no finite energy and so, neither Fourier Transform, FT, but if they have finite average power. This leads us to represent these signals by *power spectral density* that it is calculated mainly by the indirect method using the autocorrelation function. Let $x(t)$ be a random process with autocorrelation function

$$\gamma_{xx}(\tau) = E[x^*(t)x(t+\tau)] \tag{1}$$

by Winer-Khintchine theorem, the power spectral density $\Gamma_{xx}(F)$ is the FT of the autocorrelation function:

$$\Gamma_{xx}(F) = \int_{-\infty}^{\infty} \gamma_{xx}(\tau)e^{-j2\pi F\tau}dt \tag{2}$$

In a practical case, you can not know all the signal $(-\infty < t < \infty)$, and therefore we work with the autocorrelation function of time-averaged

$$R_{xx}(\tau) = \frac{1}{t_2 - t_1}\int_{t_1}^{t_2} x^*(t)x(t+\tau)dt \tag{3}$$

being $t_2 - t_1$ observation time. It is clear that the autocorrelation function equivalent to the autocorrelation function true, when $(t_2 - t_1) \to \infty$:

$$\gamma_{xx}(\tau) = \lim_{(t_2-t_1)\to\infty} R_{xx}(\tau) \tag{4}$$

Therefore through $R_{xx}(\tau)$ we can calculate an estimate of the power spectral density, which we call $P_{xx}(F)$:

$$\begin{aligned} P_{xx}(F) = \int_{-T_0}^{T_0} R_{xx}(\tau)e^{-j2\pi F\tau}d\tau = \\ \frac{1}{2T_0}\left|\int_{-T_0}^{T_0} x(t)e^{-j2\pi Ft}dt\right|^2 \end{aligned} \tag{5}$$

 ISBN: 978-84-616-2723-3

It is necessary to emphasize that we are dealing with estimates and not true values and that fulfills

$$\Gamma_{xx}(F) = \lim_{T_0 \to \infty} E[P_{xx}(F)] \tag{6}$$

Now we have to leave the analogical focus, and consider a digital environment. For a sequence $x(n)$, (from a sampled signal $x_a(t)$) of finite length N, $(0 \leq n \leq N-1)$, we can calculate the time-averaged autocorrelation as:

$$r'_{xx}(m) = \frac{1}{N-m} \sum_{n=0}^{N-m-1} x^*(n)x(n+m) \tag{7}$$

with $m = 0, 1, ..., N-1$

The estimat of the power spectral density is:

$$P_{xx}(f) = \sum_{m=-(N-1)}^{N-1} r_{xx}(m)e^{-j2\pi fm} \tag{8}$$

which leads us to the indirect method, and operating, also we obtain

$$P_{xx}(f) = \frac{1}{N}\left|\sum_{n=0}^{N-1} x(n)e^{-j2\pi fn}\right|^2 = \frac{1}{N}|X(f)|^2 \tag{9}$$

that is the direct method, and where $X(f)$ is the Fourier transform of the sequence $x(n)$.

This way of calculating the estimates of the power spectral density, is called *periodogram* [9] and is the basis for calculating the set of so-called *non-parametric methods*, remembering that is performed on the entire data record.

For a data record length L, the DFT is calculated for N points, where N is the power of 2 higher than L. This approximation $N > L$, is made by extending the data record with $N - L$ zeros in order to perform an efficient DFT calculation by FFT. This extension not adds resolution, but provides higher quality the graphical representation,due to having more points interpolated.

After calculating the FFT, the estimated power is the square of its modulus.

The resolution in frequency, is proportional to the length N of the data record. As a first approximation we can say that it is proportional to the width of the spectrum of points at -3 dB of the rectangular window, $1/N$.

In general the resolution in frequency decreases when reducing the variance of the method.

Some modifications that can be made about this method are based on the windowing of the sequence with different withdows to the rectangular window. In this case we say, that we get a modified periodogram.

 ISBN: 978-84-616-2723-3

3 Averaged of Periodograms

With this method we are looking for reducing the variance of the periodogram. It consists of dividing the data capture into smaller segments and calculate the periodogram on every one of them.

The method of averaged of periodograms was stated by Bartlett [10] and modified later by Welch [7] with the introduction of overlapping of segments and the windowing of sequences.

To enlarge registers of data whose length is L, we can proceed as follows:

- Divide the L points sequence into K segments on M points.
- Allow overlapping.
- Windowing the segments of data.
- Calculate the periodogram to every segment.
- Average the periodograms with the expression:

$$P_{xx}(f) = \frac{1}{K} \sum_{i=0}^{K-1} \tilde{P}_{xx}^{(i)}(f) \tag{10}$$

where $\tilde{P}_{xx}^{(i)}(f)$ corresponds to each of the modified periodograms by the windowing, if it was used.

Now we have K sequences of $M = L/K$ points, and because of the length of sequences is lower than those used to compute the DFT in a factor K, the spectral wide of the window increases with the same factor and so this method contributes to reduce the variance in the same K factor, but with the cost of decreasing the resolution in frequency in the same factor.

Clearly the different percentages of overlapping and different windows give rise to different variances so that in each case we must study the features that are most appropriate.

4 Results

The results presented here were obtained from a catch of 30 minutes held on January 19, 2013 at 10:14:12 hours.

 ISBN: 978-84-616-2723-3

4.1 Results of the Periodograms

The system installed at Calar Alto station records data for 30 minutes (capture time, Tc) with oversampling technique. The first sampling frequency is 52734 Hz for later by the decimation process reduces the sampling frequency down to 187 Hz. This reduces the bandwidth of interest to 93.5 Hz. The decimated process includes a low pass filter before the real decimated. In our system, both processes have been simplified in only one because we use averaging in the domain of time. The time averaging is to replace N samples by its medium value and thus filtering and decimate are performed simultaneously [11]. The time averaging can be represented as:

$$\bar{y}(t) = \frac{1}{N}\sum_{k=0}^{N-1} y(t+kT) \tag{11}$$

The registers used in our system are 30 minutes long and correspond to registers of 336600 samples. If we want to calculate the periodogram of the whole register (FFT of 2^{19} points) the resonances appear but the spectral leakage is so large that the result is not practical, see the figure 1.

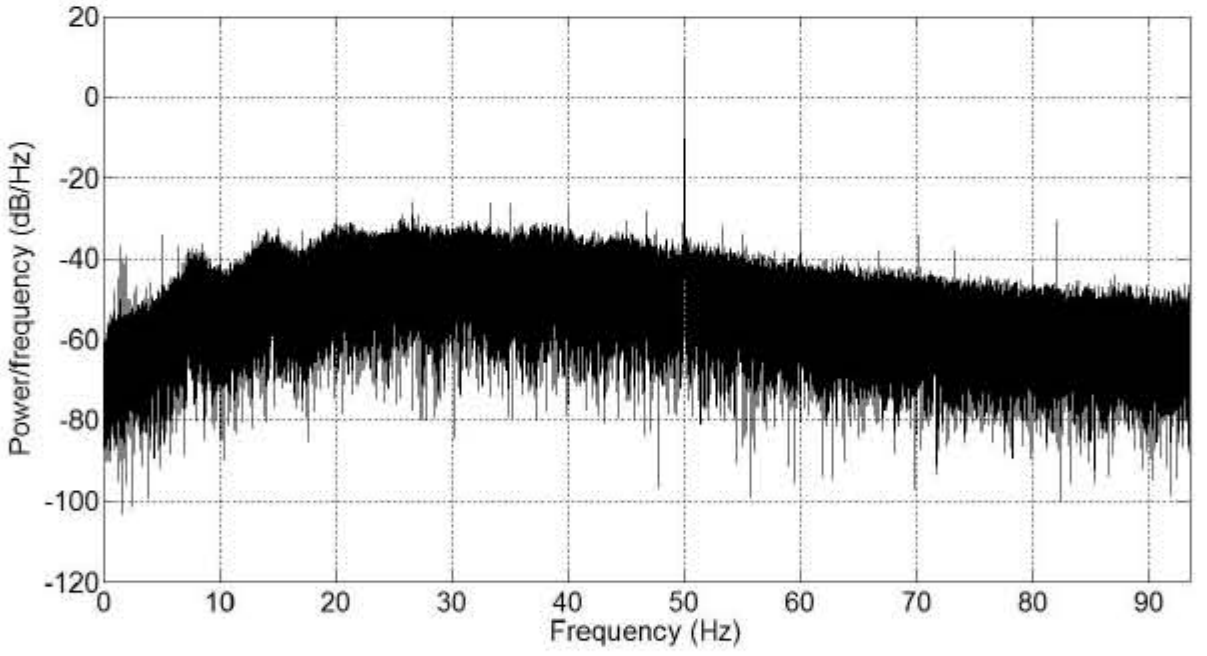

Figure 1: Capture time $Tc = 30'$. Periodogram of 336600 samples.

On the other hand if we work with small records, e.g. 10 seconds, corresponding to 1870 samples and we follow the same procedure to calculate the periodogram of the complete record (FFT of 2^{11} points) the result and the problem are identical, see the figure 2.

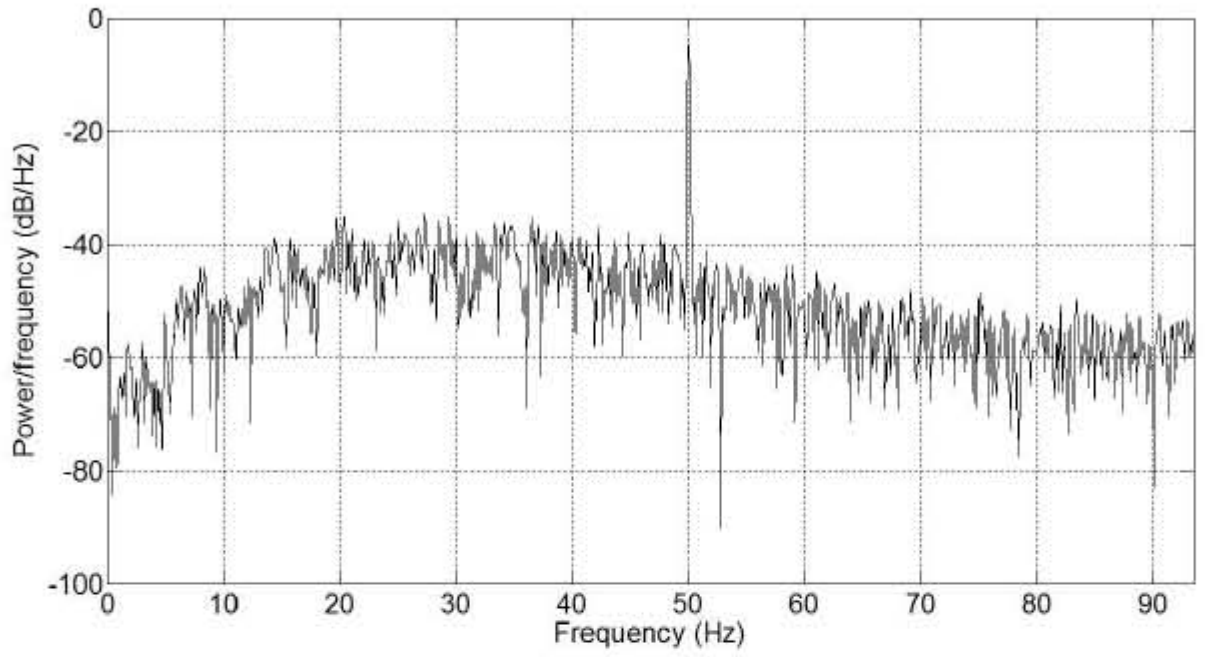

Figure 2: Capture time $Tc = 10$". Periodogram of 1870 samples.

If we compare the figures 1 and 2 we can observe the effects of the spectral leakage and the effects of the frequency resolution. The frequency resolution $(1/L)$ is proportional to the length of the record, and we can see that in figure 1 (high spectral resolution) spectral lines appear and these are not shown in figure 2 (low spectral resolution).

4.2 Results of averaged Periodograms

After several tests with data records of different capture times and different number of samples we can compare the results in the following figures:

The tests were performed on the same capture using the first 2 minutes, the first 5 minutes and complete record of 30 minutes. In both cases they were divided into record segments of 187 samples (1 second) and 1870 samples (10 seconds) resulting in different amounts of segments and therefore number of averages:

- Capture time $Tc = 2$ minutes. Record length $L = 22440$ samples
  - Number of segments $K = 120$. Segment length $M = 187$ samples. Figure 3.
  - Number of segments $K = 12$. Segment length $M = 1870$ samples. Figure 4.

 ISBN: 978-84-616-2723-3

- Capture time $Tc = 30$ minutes. Record length $L = 336600$ samples
  - Number of segments $K = 1800$. Segment length $M = 187$ samples. Figure 5.
  - Number of segments $K = 180$. Segment length $M = 1870$ samples. Figure 6.

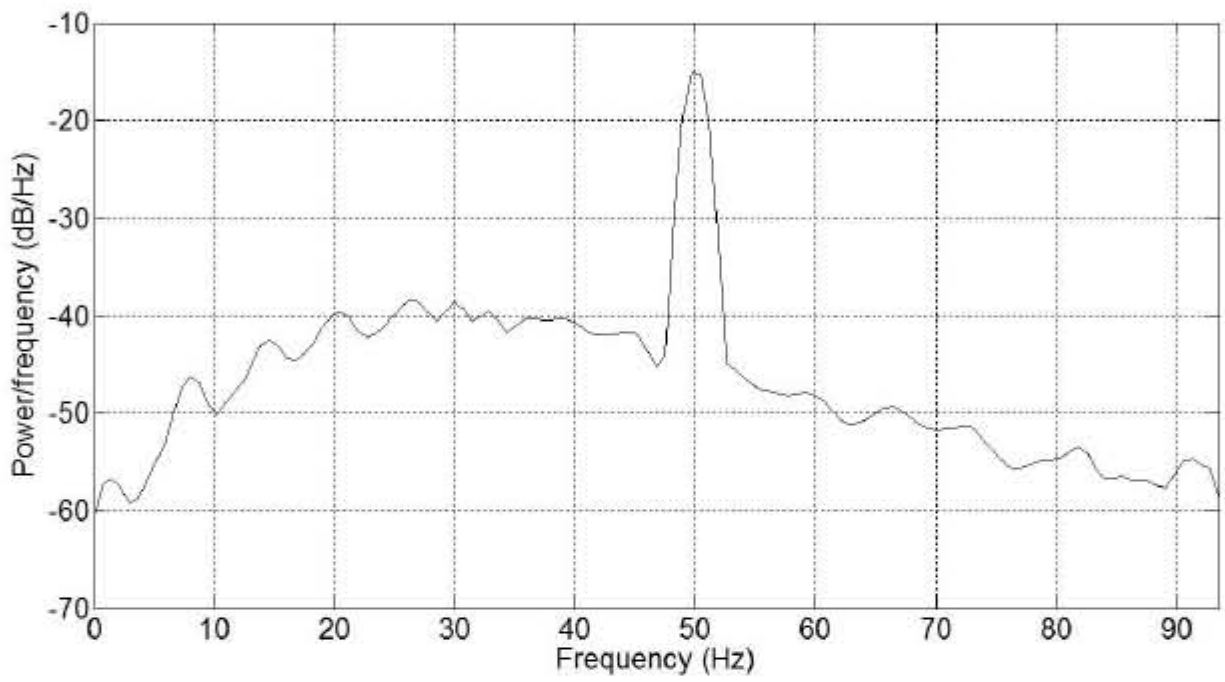

Figure 3: $Tc = 2$', $L = 22440$, $M = 187$, $K = 120$.

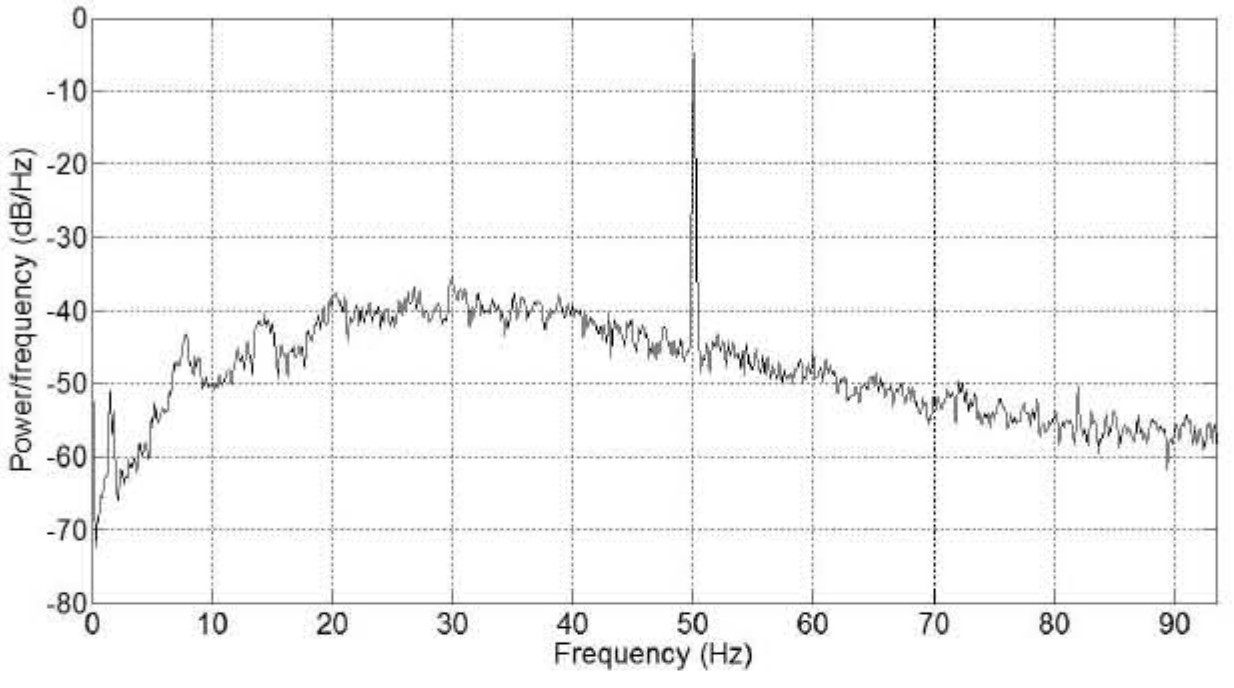

Figure 4: $Tc = 2$', $L = 22440$, $M = 1870$, $K = 12$.

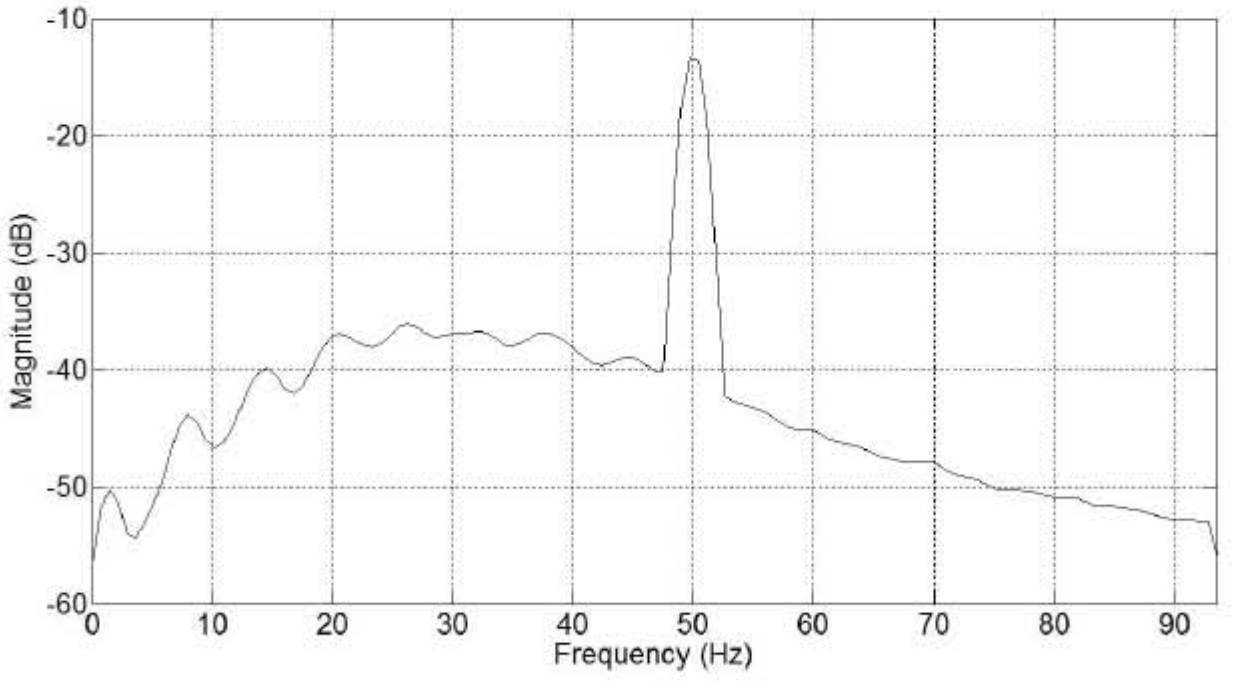

Figure 5: $Tc = 30$', $L = 336600$, $M = 187$, $K = 1800$.

 ISBN: 978-84-616-2723-3